Article

Spectroscopic, Electrochemical and DFT Studies of Phosphorescent Homoleptic Cyclometalated Iridium(III) Complexes Based on Substituted 4-Fluorophenylvinyl- and 4-Methoxyphenylvinylquinolines

Adewale O. Adeloye [1,*], Malose J. Mphahlele [1] iD **, Abolanle S. Adekunle [2], Lydia Rhyman [3]** iD **and Ponnadurai Ramasami [3]**

[1] Department of Chemistry, College of Science, Engineering and Technology, University of South Africa, Private Bag X6, Florida 1710, South Africa; mphahmj@unisa.ac.za
[2] Department of Chemistry, Faculty of Science, Obafemi Awolowo University, Ile-Ife, Nigeria; aadekunle@oauife.edu.ng
[3] Computational Chemistry Group, Department of Chemistry, Faculty of Science, University of Mauritius, Réduit 80837, Mauritius; lyd.rhyman@gmail.com (L.R.); ramasami@uom.ac.mu (P.R.)
* Correspondence: aowale@gmail.com; Tel.: +26-775-127-465

Abstract: This study reports the synthesis and comparative investigation of the substituent effects of a new series of highly luminescent homoleptic tris-cyclometalated iridium(III) complexes of the type $[Ir(N^{\wedge}C)_3]$. These are based on two ligand type derivatives comprising of 4-fluorophenylvinylquinolines and 4-methoxyphenylvinylquinolines with electron-donating and/or electron-withdrawing groups as aryl substituents at 2-position. The structures of the ligands and their complexes were characterized by means of FT-IR, UV-Vis and NMR spectrometry complemented with photoluminescence and cyclic voltammetry. The photophysical properties of 2-aryl-4-(4-fluorophenylvinyl)quinoline and its corresponding complex were also studied using the density functional theory method. The photoluminescent properties of the ligands and the corresponding complexes showed high fluorescent intensities and quantum yields in solvents of different polarities. The photoluminescence spectra of the complexes in solid film, showed common transmission curves at longer wavelengths maximum (λ_{em} = 697 nm) possibly originating from the interference of scattered light of higher-order transmission of monochromators.

1. Introduction

In the past few years, luminescent cyclometalated iridium(III) complexes have continued to attract significant attention. The studies involving the photophysical and electrochemical properties of iridium coordination and organometallic complexes have gathered much interest. The reasons for such an interest are due to their strong metal-ligand bonding interactions as well as their ability to emit light from both singlet and triplet excitons leading to high chemical photostability, which allows continuous exposure of the complexes to irradiation, long emission lifetimes, and large Stokes' shifts [1–13]. The tuning of the second-order nonlinear optical (NLO) response of the unusual family of 3D chromophores of certain cyclometallated Ir(III) complexes with appropriate ligand substitution has allowed contribution to their interesting luminescent properties [14]. A correlated investigation

of the photoluminescent and electroluminescent properties at different bias voltages of iridium(III) ionic transition metals complexes (Ir-iTMC), for example, has been shown to be dependent on the applied electric field. Increased bias voltage leads to Electroluminescent (EL) spectrum dominated by red-shifted components that are related to the morphological rearrangement of the materials due to enhanced local electric field. The overall effect is the contribution to degradation and changes in the spectral behavior of the electroluminescent and photoluminescent decay times [14–18]. The development of pure-blue-to-deep-blue-emitting ionic phosphors is an ultimate challenge for full-colour displays and white-light sources in the field of optoelectronics. However, it has been reported that the control of the frontier orbital energy level (HOMO-LUMO, Highest Occupied Molecular Orbital-Lowest Unoccupied Molecular Orbital) is the sole method to achieve better blue phosphorescent iridium complexes by appropriate ligand selection and the introduction of adequate substituents [19].
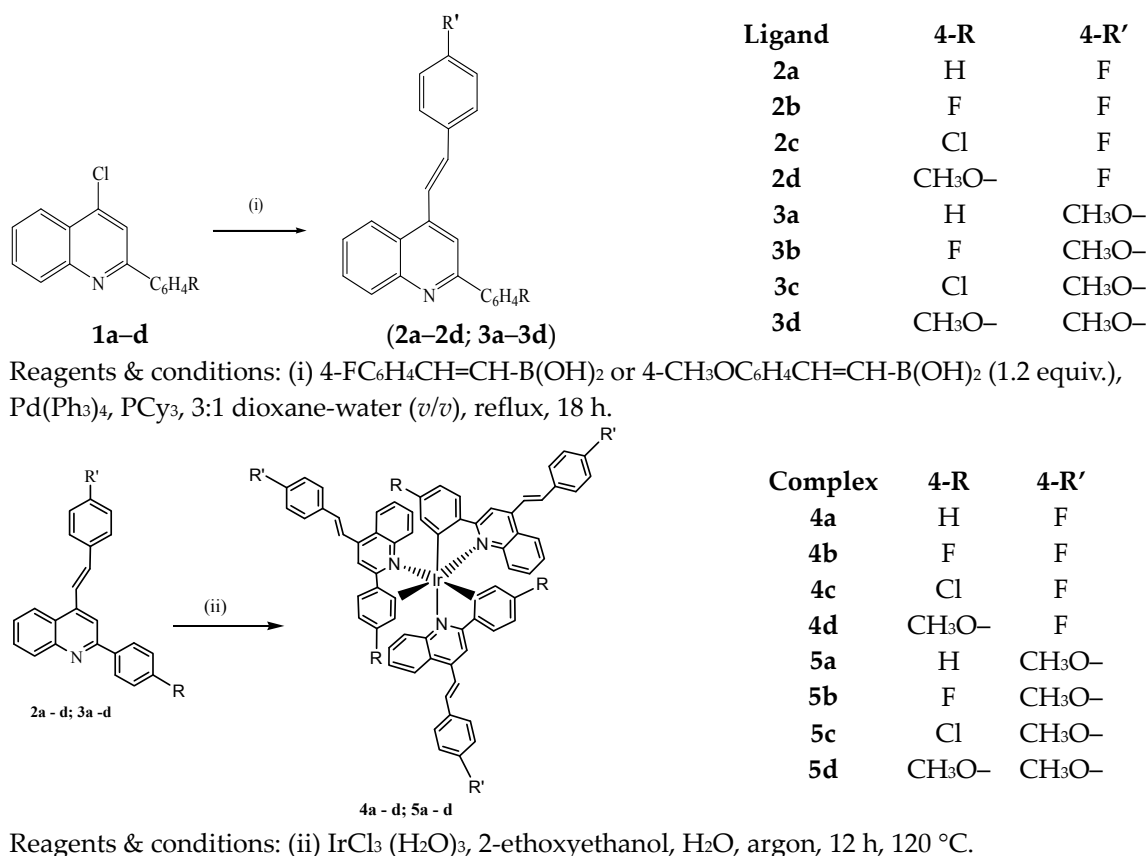
Based on the synthesis of cyclometalated Ir(ppy)$_3$ (where ppy represents 2-phenylpyridine), which has been extensively investigated as a green material for Organic Light Emitting Diodes (OLEDs), a strong emission originates from the triplet excited states having both the $\pi \rightarrow \pi^*$ and metal-to-ligand-charge-transfer (MLCT) characteristics. Several methods have been employed in order to tune the emission to the red region of the spectrum. The elongation of conjugative bonds in molecules, replacement of one CH– group at the pyridyl ring of phenylpyridine ligand by nitrogen, doping of cyclometalated iridium complexes into a host thus given control of the intermolecular interaction, introduction of dendrimers due to their three-dimensional hyper branched structural types into the molecular structures and the addition of either electron-donating or electron-withdrawing functional groups to the pyridyl ring and the phenyl ring, respectively, were among the methods used for wavelength enhancement [20–28].

In this paper, we report the synthesis, characterization and comparative studies of eight novel highly luminescent 4-fluorophenylvinylquinolines (**2a**–**d**) and 4-methoxyphenylvinylquinolines (**3a**–**d**) ligands containing both electron donating and withdrawing groups particularly as aryl-substituents at 2-position of the quinoline scaffold and their corresponding homoleptic cyclometalated iridium(III) complexes of the type [Ir(N$^\wedge$C)$_3$]. The molecular rearrangement of the different substituents on quinoline ligands reflects the general changes in the photophysical and electrochemical properties of the compounds. We complemented this study using the density functional theory (DFT) method on one of the ligands, namely 2-aryl-4-(4-fluorophenylvinyl)quinoline and its corresponding complex.

2. Results

2.1. Synthesis

The synthesis of the reported compounds first involves the use of the 2-aryl-4-chloroquinolines (**1a**–**d**) as substrates for palladium-catalyzed Suzuki cross-coupling with 4-(fluorophenylvinyl)boronic acid and 4-(methoxyphenylvinyl)boronic acid (1.2 equiv.) as coupling partners in the presence of Pd(PPh$_3$)$_4$–PCy$_3$ catalyst complex as Pd(0) source and potassium carbonate as a base in 3:1 dioxane-water mixture (*v/v*) under reflux (Scheme 1) [29]. The prepared 2-aryl-4-(4-fluorophenylvinyl)quinolines (**2a**–**d**) and 2-aryl-4-(4-methoxyphenylvinyl)quinolines (**3a**–**d**) were used in this investigation as models for comparative studies in the electronic absorption and emission properties, and a further electrochemical studies for the corresponding homoleptic Ir(III) complexes of the type [Ir(N$^\wedge$C)$_3$], coded as **4a**–**d** and **5a**–**d**, respectively. The structure of the prepared complexes was characterized by means of ^{1}H NMR spectroscopy and elemental (C/H/N) analysis. The coordinates for the optimised structures of the ligand **2a** and the corresponding complex **4a** in the gas phase are provided as Supplementary Materials (Tables S1 and S2, respectively). Table 1 summarizes the selected bond lengths (Ir–N and Ir–C) of the complex (**4a**). The literature values of these bond lengths of compounds with quinoline moiety are also included in the table, and it is observed that there is a good comparison.

Ligand	4-R	4-R′
2a	H	F
2b	F	F
2c	Cl	F
2d	CH₃O–	F
3a	H	CH₃O–
3b	F	CH₃O–
3c	Cl	CH₃O–
3d	CH₃O–	CH₃O–

Reagents & conditions: (i) 4-FC₆H₄CH=CH-B(OH)₂ or 4-CH₃OC₆H₄CH=CH-B(OH)₂ (1.2 equiv.), Pd(Ph₃)₄, PCy₃, 3:1 dioxane-water (*v/v*), reflux, 18 h.

Complex	4-R	4-R′
4a	H	F
4b	F	F
4c	Cl	F
4d	CH₃O–	F
5a	H	CH₃O–
5b	F	CH₃O–
5c	Cl	CH₃O–
5d	CH₃O–	CH₃O–

Reagents & conditions: (ii) IrCl₃ (H₂O)₃, 2-ethoxyethanol, H₂O, argon, 12 h, 120 °C.

Scheme 1. Suzuki cross-coupling of the 2-aryl-4-chloroquinolines **1a–d** with arylvinylboronic acids.

Table 1. Selected bond lengths (Ir–N and Ir–C) in Å of complex **4a** and their comparison with literature values.

	4a	Literature [30]
Ir–N	2.299	2.173
Ir–C	2.018	2.017

2.2. Electronic Absorption and Luminescence Spectra of Ligands

2.2.1. Electronic Absorption of Ligands

As a prelude to compounds with potential photoelectronic properties, the absorption spectra of the ligands were investigated in solution at room temperature (RT). The electronic absorption of the compounds **2a–d** and **3a–d** measured in chloroform are shown in Figures 1 and 2 and summarized in Table S3 (see Supplementary Materials). The strong absorption maxima wavelength bands in the region λ_{abs} = 261–297 nm in the ultraviolet region areas were assigned to the spin-allowed ligand-centered (¹LC) $\pi \rightarrow \pi^*$ transitions and the bands in the region λ_{abs} = 320–354 nm also assigned to the $\pi \rightarrow \pi^*$ intramolecular charge transitions (ICT), which possibly originate from further conjugation made by the electron donor and electron acceptor species present in the cyclometalated ligands. The types and positions of the substituents were found to have strong effects on the molar extinction coefficients (ε) and wavelengths (λ_{abs}) of the compounds [31–33]. By comparison, ligands **2a** and **3a** with a phenyl substituent at position 2 of the quinoline framework showed no apparent change in the molar extinction coefficient, as the wavelengths almost close to each other. Clear distinctions of the molar extinction coefficient were, however, observed with the 2-aryl-4-(4-fluorostyryl)quinolines **2b–d** and 2-aryl-4-(4-methoxystyryl)quinolines **3b–d** substituted at the *para*-positon of the 2-aryl ring

with a strong electron withdrawing halogen atom (F, Cl) and strong electron donating methoxy group. A red-shift in wavelength maxima was observed **2b** (λ_{abs} = 278 nm) and **2d** (λ_{abs} = 293 nm) substituted with 2-(4-fluorophenyl)- and 2-(4-methoxyphenyl)- group, respectively. On the other hand, a blue-shift in wavelength to λ_{abs} = 267 nm was observed for **2c** substituted with a 2-(4-chlorophenyl) group. By comparison, in the red region of absorption, compounds **2a–c** and **3a–c** showed a corresponding steady increase in wavelength maxima at (λ_{abs} = 335, 337 and 328 nm) and (λ_{abs} = 340, 354 and 348 nm), respectively. No apparent change was observed in the wavelength maxima for **2d** and **3d** at (λ_{abs} = 338 nm). DFT computation in chloroform indicates that the most intense peak appears at λ_{abs} = 362 nm (experiment, λ_{abs} = 335 nm) with an oscillator strength of 0.595, and this is assigned to HOMO to LUMO transition. The HOMO-LUMO gap of ligand (**2a**) is 3.82 eV in chloroform. Similar patterns in the absorption wavelengths were observed in the analogues' derivatives **3b**, **3c** and **3d** at λ_{max} = 354, 348 and 338 nm, respectively. However, significant changes in spectral pattern and reduced molar extinction coefficient generally characterized the ligands **3b**, **3c** and **3d** than those of **2b**, **2c**, **2d** with exception in **3c**, which showed significant hyperchromic effect. It has been reported that an increase in the wavelength as observed for the 4-methoxyphenyl substituents plays a useful role in the energy gap determination between the highest occupied molecular orbital (HOMO) and the lowest unoccupied molecular orbital (LUMO) [28]. It is well known that consideration of the electronic effects has been shown to have a significant influence on orbital energies and the relative ease with which electron-withdrawing (e.g., –F, –CF$_3$) and electron-donating (e.g., –(CH$_3$)$_3$, –OCH$_3$) groups can be incorporated into the ligand structure. Accordingly, electron-withdrawing substituents tend to stabilize the HOMO by removing electron density from the metal, whereas donating groups have an inverse effect [34–38]. This relationship is complicated by the fact that electron withdrawing groups may also lower the energy of the LUMO (i.e., increasing the electron affinity of the parent ligand).
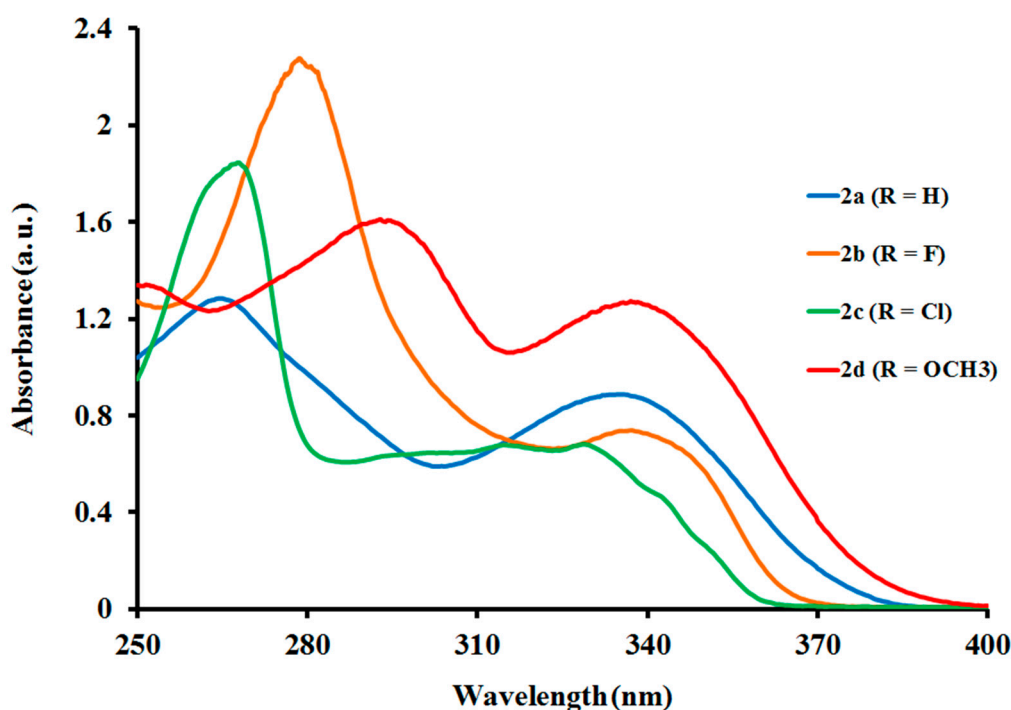

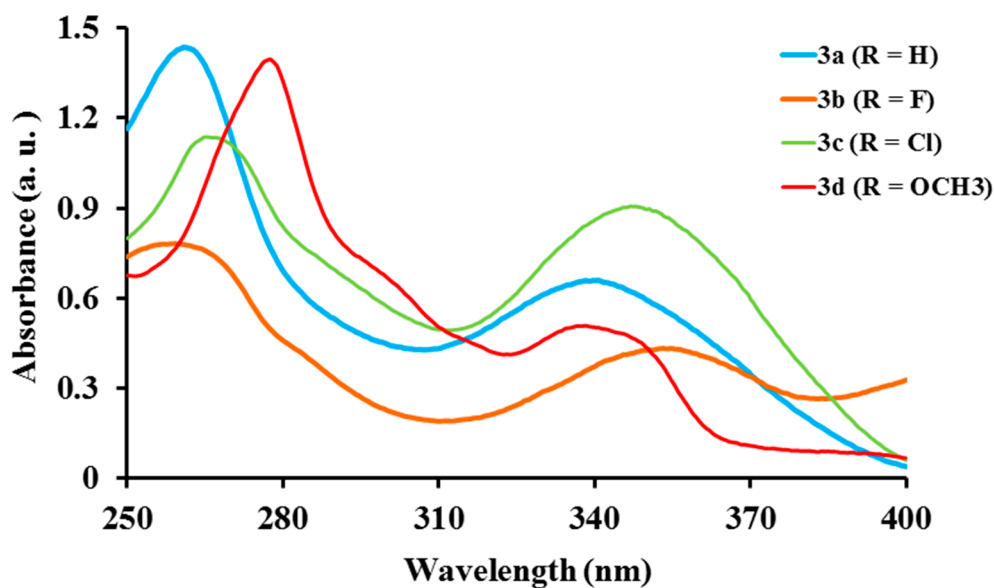**Figure 1.** UV-Vis Absorption spectra of (**2a–d**) in chloroform (concentration 1.0 × 10^{-3} mol/L).

Figure 2. UV-Vis absorption spectra of **3a–d** in chloroform (concentration 1.0×10^{-3} mol/L).

2.2.2. Photoluminescence Properties of Ligands

The emission properties of the ligands were investigated in three different solvents of varying polarities at excitation wavelengths in the region λ_{ex} = 350–385 nm. Highly intense photoluminescence (PL) with a similar pattern characterized by single emission bands were observed for the ligands **2a–d** and **3a–d** in chloroform and methanol with λ_{em} values located in the regions 449–478 nm and 455–470 nm, respectively (Figures 3 and 4). These values in dimethyl formamide solution are located in the region λ_{em} at 406–442 nm (see Figure 3b) for **2a–d** and λ_{em} 389–454 nm for **3a–d** (refer to Figure 4b). The effects of the position or type of substituents on quinoline framework were particularly observed in the 2-(4-halogenophenyl)-4-(4-fluorostyryl)quinolines **2b** and **2d**, and the analogous 2-(4-halogenophenyl)-4-(4-methoxystyryl)quinolines **3b** and **3d**. In chloroform or methanol solutions, **2b** with a combination of 2-(4-fluorophenyl)- and 4-(4-fluorostyryl) moieties was found to exhibit lower emission value at λ_{em} = 454 and 439 nm, respectively. Compound **3d** with a combination of the 2-(4-methoxyphenyl)- and 4-(4-methoxystyryl) groups was found to emit at λ_{em} = 455 and 470 nm. Likewise, a combination of 2-(4-methoxyphenyl)- and 4-(4-fluorostyryl) groups in **2b** or 2-(4-fluorophenyl)- and 4-(4-methoxystyryl) groups in **3b** resulted in the highest emission wavelength at λ_{em} = 478 and 482 nm or λ_{em} = 470 and 481 nm, respectively [26]. Interestingly, the nature and position of the substituents on the aromatic rings did not show any significant effect on the wavelength shifts between **2d** and **3b** in the polar protic methanol. Accordingly, the quinoline framework is expected to be made more electron-deficient as a result of the formation of strong solute–solvent interaction through intermolecular hydrogen bond with N-1 as expected from the strong protic methanol [28]. On the other hand, in the DMF solution, the effect of the electron-withdrawing groups increases the emission intensity steadily between the 4–FC_6H_4- and the 4–ClC_6H_4- group and the trend is as follows: **2c** > **2b** > **2a**. However, this effect is of a lesser extent when compared to the electron-donating methoxy group in **2d** with a bathochromic shift in emission wavelength (Figure 3b). On the other hand, the emission intensities of compounds **3a–d** were significantly reduced and followed the trend **3a** > **3b** > **3c** with a blue-shift in emission wavelength of about 53 nm in **3d** compared to **2d** (Figure 4b).
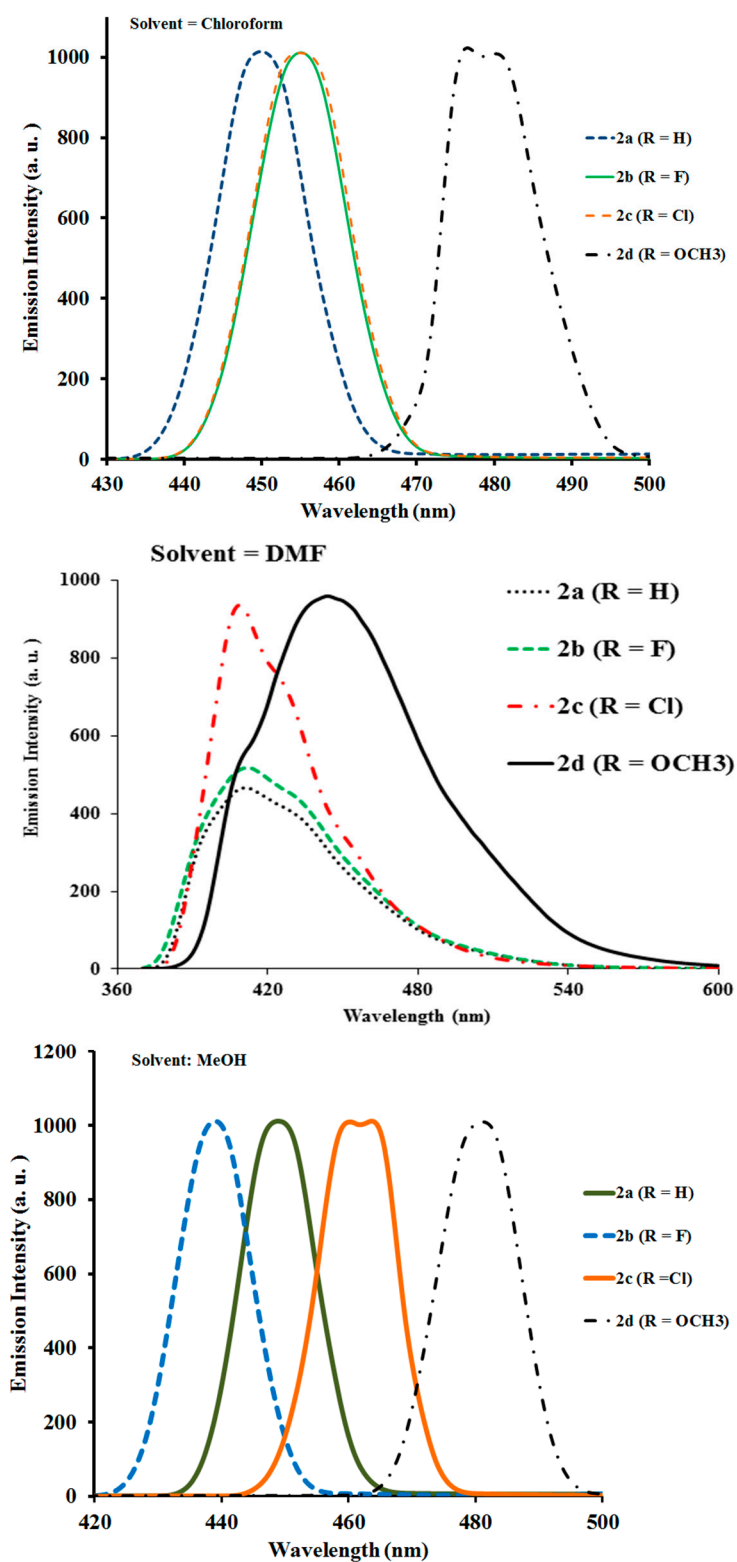
Figure 3. Fluorescence emission spectra of **2a–d** (concentration 2.0×10^{-7} mol/L) at RT (room temperature).
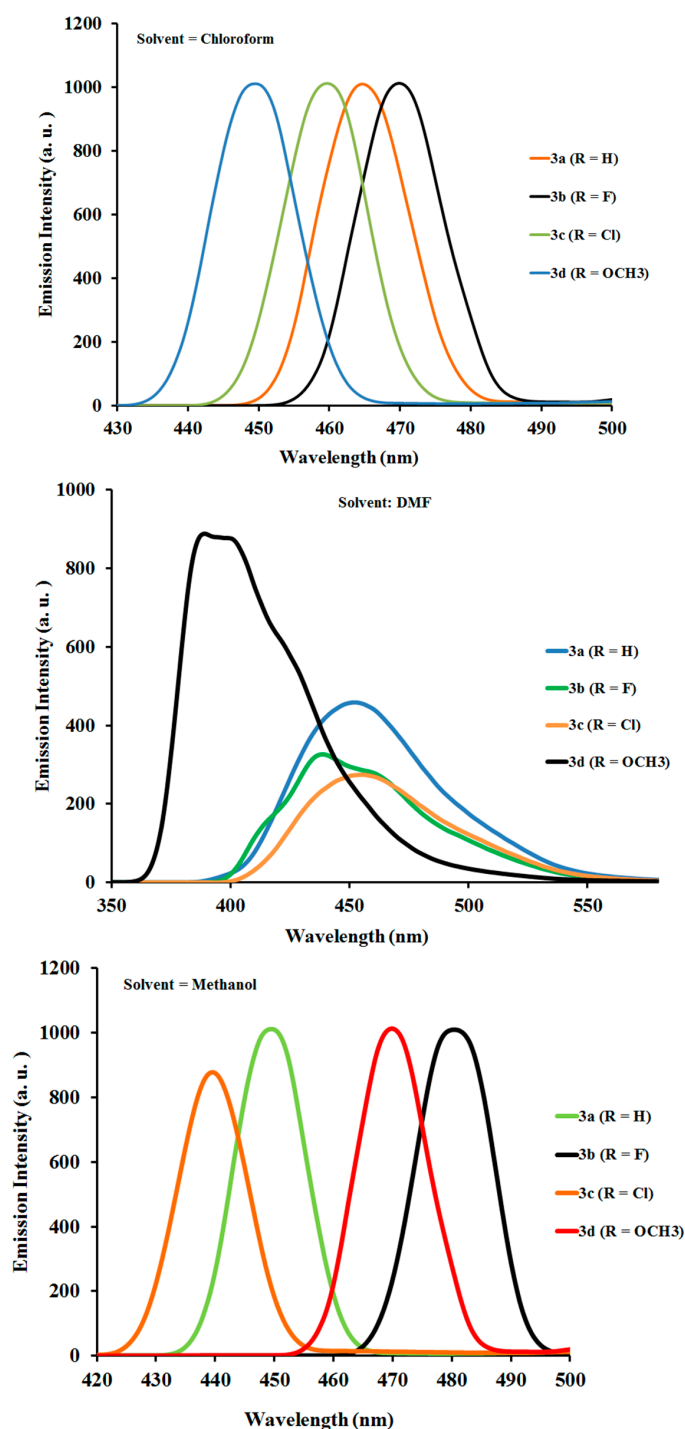
Figure 4. Fluorescence emission spectra of **3a–d** (concentration 2.0×10^{-7} mol/L) at RT.

2.3. Electronic Absorption and Luminescence Spectra of Complexes

2.3.1. Electronic Absorption of Complexes

The electronic absorption spectra of the homoleptic Ir(III) cyclometalated complexes **4a–d** and **5a–d** obtained from ligands **2a–d** and **3a–d** and recorded at room temperature in methanolic solution are shown in Figures 5 and 6, respectively, and the corresponding data is summarized in Table S4 in the Supplementary Materials. All of the complexes showed intense spin-allowed intraligand (^{1}IL) absorption bands at the higher energy region λ_{max} = 261–300 nm (ε on the order of

10^4 dm^3 mol^{-1} cm^{-1}), which are attributed to the $\pi \to \pi^*$ transitions and the intramolecular charge transfer transitions due to derivatized quinoline framework. The less intense low-lying absorption bands were in the range λ_{max} 335–397 nm for Ir(III)-(**4a–d**) and λ_{max} 348–384 nm for Ir(III)-(**5a–d**) complexes. These bands are attributed to the spin-allowed metal-to-ligand charge transfer (^{1}MLCT) ($d\pi$(Ir)$\to\pi^*$(N^C) transitions, although assumed to be possibly mixed to a certain extent, with ligand-centered $\pi \to \pi^*$ transitions to form metal-to-ligand-ligand charge transfer (MLLCT) [39]. On the other hand, the spin-forbidden metal-to-ligand charge transfer band (^{3}MLCT) transitions appear as weak shoulder bands at lower energy absorption in the λ_{max} region 450–500 nm, which may be attributed to ($d\pi$(Ir)$\to\pi^*$(N^C) transitions [40]. The most intense peak of complex (**4a**) in methanol is observed at λ_{max} = 378 nm or 3.28 eV with an oscillator strength of 0.7374, and this is assigned mostly to HOMO-4 to LUMO transition. The HOMO-LUMO gap is 2.99 eV, and this gap is in agreement with analogous iridium complexes reported in the literature [41].
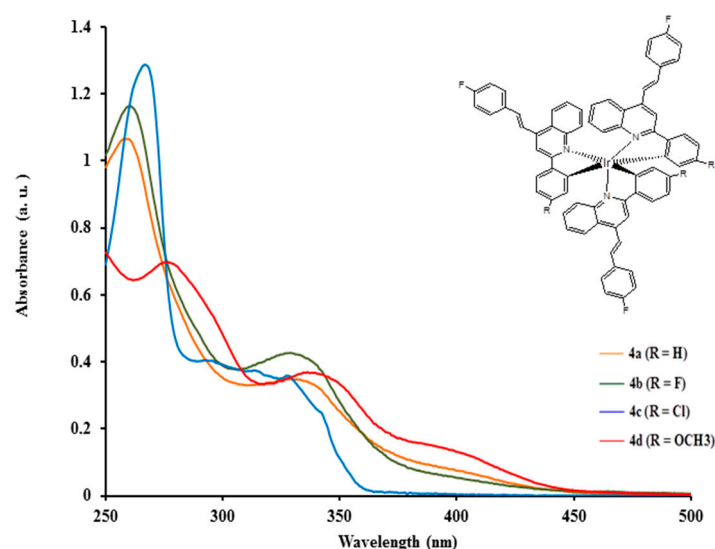

Figure 5. UV-Vis Absorption spectral of Ir(III) complexes **4a–d** in methanol (concentration 1.0×10^{-3} mol/L).
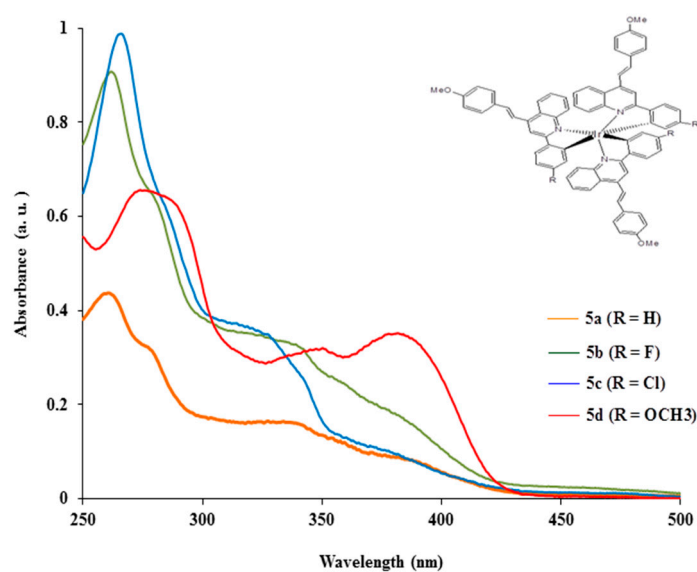

Figure 6. UV-Vis Absorption spectral of Ir(III) complexes of **5a–d** in methanol (concentration 1.0×10^{-3} mol/L).

As observed in Figure 5, the introduction of 4-(4-fluorophenylvinyl) group on the quinoline framework and the presence of a 2-(4-halogenophenyl) ring lead to increased molar extinction coefficients at the higher energy region of the spectra as compared to those for 2-phenyl- and 2-(4-methoxyphenyl)substituted derivatives in the trend **4c** > **4b** > **4a** > **4d**. The absorption wavelength maxima for these complexes tend towards the lower energy region and the trend is reversed as follows: **4d** > **4a** > **4b** > **4c**. Complex **4c** with a 2-(4-chlorophenyl) substituted 4-(4-fluorostyryl)quinoline framework does not exhibit appreciable MLCT absorption band in the wavelength region longer than λ_{max} = 360 nm. Complexes **4a**, **4b** and **4d**, on the other hand, have absorption extended to about λ_{max} = 445 nm, which may be due to the forbidden ^{3}MLCT transition of the complexes. It is well known in the literature that molecules with intramolecular donor–acceptor (DA) systems exhibit bathochromic shifts of both absorption and emission spectra [21]. A low ^{1}MLCT absorption band was recorded for complex **4c**, and the reason for this anomalous behavior is not clear to us at this stage. The characteristics of the absorption wavelengths were strongly influenced when the substituent on the 4-position of the quinoline scaffold is the 4-methoxyphenylvinyl functionality with variations in the *para*-position of the 2-aryl group incorporating the electron-donating or electron-withdrawing substituents as shown in Figure 6. The absorption spectra of complexes **5a–d** when compared to those of **4a–d** counterparts (see Figure 5) showed absorption wavelengths for **5b** and **5c** containing the 4-(halogenophenyl) rings at the 2-position. These two complexes maintained their higher molar extinction coefficient values at the higher energy levels as compared to other complexes containing the 2-phenyl or 2-(4-methoxyphenyl) substituted quinoline scaffolds with the following trend **5c** > **5b** > **5d** > **5a**. However, in a similar fashion, as the absorption bands tend towards the lower energy region of spectra, the molar extinction coefficients of the halogenophenyl group decrease steadily in the trend **5d** > **5b** > **5c** > **5a**. Clear and significant reduction in molar extinction coefficient was observed for **5a** (ε = 0.27 $\times$ 10^4 M^{-1} cm^{-1}) having only phenyl ring at the 2-position of the quinoline framework as compared to **5d** with 4–OCH$_3$ (ε = 0.61 $\times$ 10^4 M^{-1} cm^{-1}). It has previously been established that an electron-donating group can influence the highest occupied molecular orbital (HOMO) and/or the lowest unoccupied molecular orbital (LUMO) level as well as ^{1}MLCT state of the iridium(III) complex [32].

2.3.2. Photoluminescent Properties of Complexes

Photoluminescent properties of the complexes **4a–d** and **5a–d** were investigated both in methanolic solution as well as in the solid state at room temperature. Figures 7–10 show the luminescence spectra of the Ir complexes and summary of data reported in Table S4 in the Supplementary Materials. All of these complexes emit intense phosphorescence bands with λ_{em} values ranging from 470 nm to 545 nm in solution, which corresponds to blue-green light [39–41]. In comparison to complexes containing 4-(4-fluorophenylvinyl)quinoline as the common substituent group as shown in Figure 7, complex **4b** having 2-(4-fluorophenyl) group exhibits the highest emission wavelength at λ_{em} = 530 nm, followed by the 2-phenyl substituted complex **4a** at λ_{em} = 499 nm. A further blue-shift in wavelengths was observed at λ_{em} = 489 nm or at λ_{em} = 470 nm for **4c** or **4d** bearing the 2-(4-chlorophenyl) or 2-(4-methoxyphenyl) group, respectively. As shown in Figure 8, no appreciable changes in wavelengths were observed for the 2-phenyl- **5a**, 2-(4-flurophenyl) **5b** and 2-(4-chlorophenyl) substituted derivative **5c**. However, moderate red-shift in wavelength at λ_{em} = 545 nm was observed for **5d** having strongly electron-donating 2-(4-methoxyphenyl) and 4-(4-methoxystyryl) groups on the quinolone framework. As previously accounted for in the ligands, it may be assumed possibly that strong solute–solvent interaction through intermolecular hydrogen bond with N-1 as expected from the strong protic methanol solvent effect plays a major role in the enhancement of luminescent properties of the strong electron-donating 4-methoxyphenyl and 4-methoxystyryl groups on the quinoline ring system for these complexes. A common interesting feature among the two series of complexes **4** and **5** is the observed lower emission intensity exhibited by the 2-(4-chlorophenyl)quinoline–based complexes **4c** and **5c**. The decrease in emission intensity may be due to the heavy atom effect of chlorine, which increases the probability of the intersystem crossing as the size of the molecule increases [42].
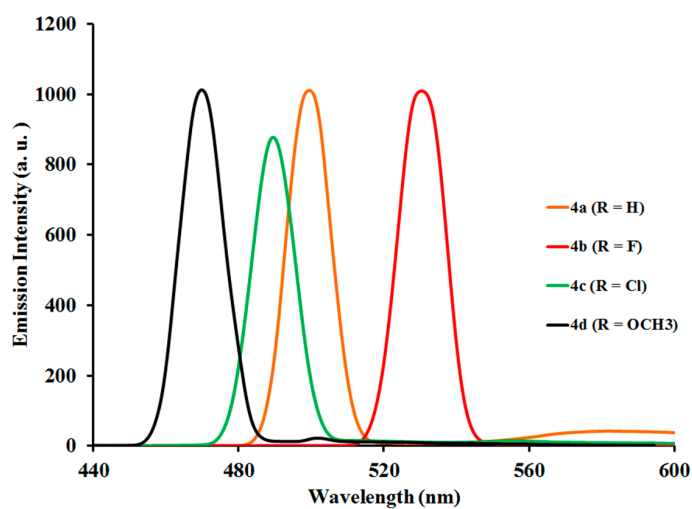
Figure 7. Phosphorescence emission spectra of (Ir(**4a–d**)$_3$) at λ_{ex} = 350 nm in methanol (concentration 2.0×10^{-7} mol/L) at RT.
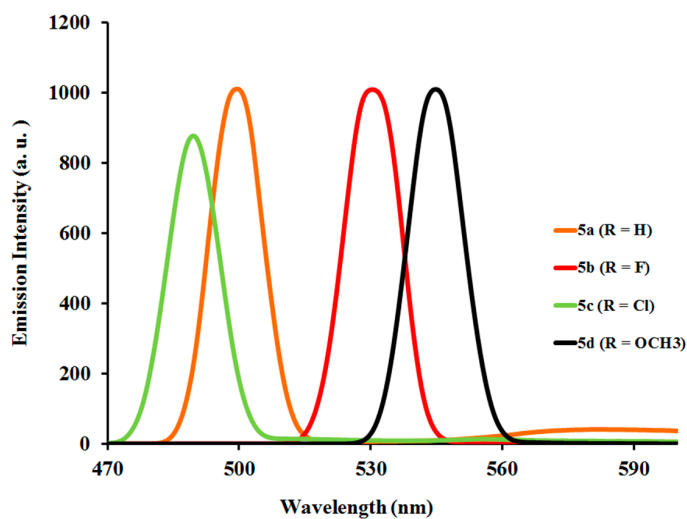
Figure 8. Phosphorescence emission spectra of (Ir(**5a–d**)$_3$) at λ_{ex} = 350 nm in methanol (concentration 2.0×10^{-7} mol/L) at RT.
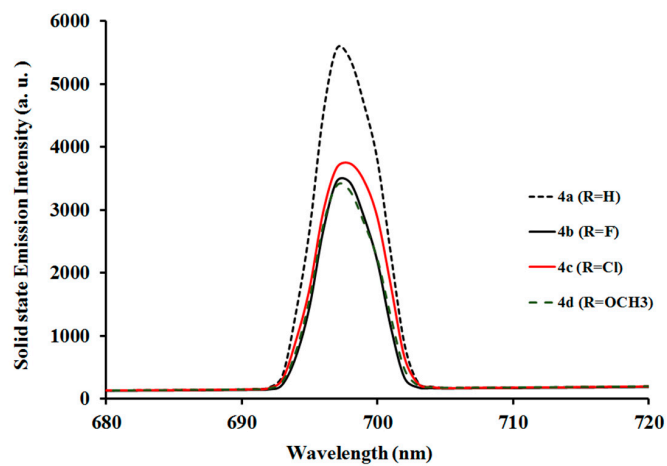

Figure 9. Solid state phosphorescence emission spectra of (Ir(**4a–d**)$_3$) at λ_{ex} = 350 nm at RT.

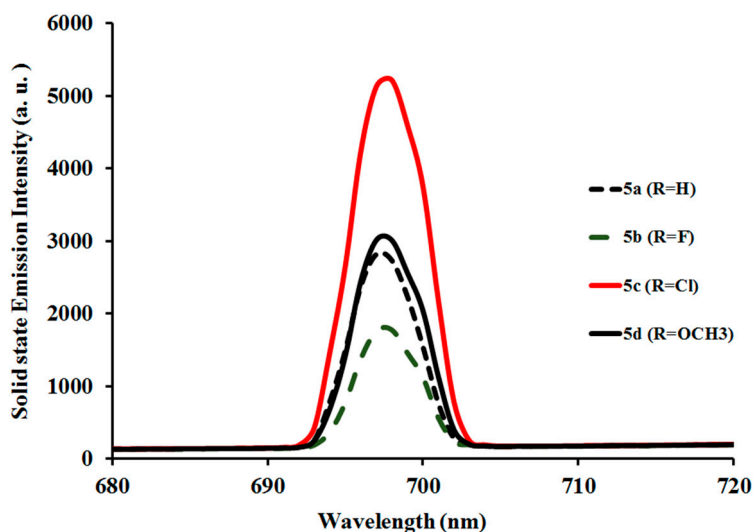**Figure 10.** Solid state phosphorescence emission spectra of (Ir(**5a–d**)₃) at λ_{ex} = 350 nm at RT.

It is interesting to note that, under photoexcitation in the solid state, all of the Ir(III) complexes tuned the emission from the green to red light as shown (Figures 9 and 10) compared to those in methanolic solution. All complexes emit at a common wavelength of λ_{em} = 697 nm with varied emission intensities. It has been reported that emission becomes more dominant in the solid state when more efficient energy transfer obtained from intermolecular energy transfer from the ligand to the complex are induced by shorter intermolecular distance in the solid state [41]. These emission profiles were envisioned to originate from the ligand-centred excited state, metal-centred excited state, and the MLCT excited state, since in the cyclometalated Ir complexes, the wave function of the excited triplet state, Φ_T, responsible for phosphorescence is principally expressed to be:

$$\Phi_T = a \times \Phi(LC)_T + b \times \Phi(MLCT)_T,$$

where a and b are the normalized coefficients and $\Phi(LC)_T$ and $\Phi(MLCT)_T$ are the wave functions of the ligand-centred ($^3\pi$–π^*) and the MLCT excited triplet state, respectively. Accordingly, the above equation showed that the excited triplet states of the iridium complexes are a mixture of $\Phi(LC)_T$ and $\Phi(MLCT)_T$, whereas, the triplet excited state is attributed to the dominantly $^3\pi$–π^* excited state when a > b and the dominantly ^{3}MLCT excited state when b > a [21,39,43–49]. The emission curves may be the product of transmission at longer wavelengths, which originated due to the interference from scattered light made possible through the higher-order transmission of monochromators. This would probably account for the observed reduction in emission intensities of the complexes **4a–d** and **5a–d** at higher excitation wavelengths 400 nm and 450 nm (not shown). The optical density of the samples due to sample preparation and concentration errors may also have contributed to the distortion of the emission spectra if the linear range of about 0.1 absorbance units is exceeded leading to intensity fluctuations as particles drift through the laser beam [50–52].

The phosphorescence spectra of the Ir complexes of **4a–d** shown in Figure 9 reveal the highest emission intensity for **4a** bearing a 2-phenyl ring. A slightly higher emission intensity was observed for the 2-(4-chlorophenyl)–substituted complex **4c** as compared to the analogous 2-(4-fluorophenyl)–substituted complex **4b**. The 2-(4-methoxyphenyl)–substituted complex **4d** was found to exhibit the lowest emission intensity than the other derivatives. Figure 10 shows the solid state phosphorescence emission spectra of complexes **5a–d**. The highest emission intensity was observed for complex **5c** with a 2-(4-chlorophenyl) and 4-(4-methoxystyryl) groups around the quinoline core. Within this series, complex **5b** with a 2-(4-fluorophenyl) group on the 4-methoxystyrylquinoline exhibits the lowest emission intensity than the other derivatives. Complexes **5a** and **5d** only

showed moderate emission intensity. The presence of the 2-(4-fluorophenyl) substituent on the 4-(4-fluorostyryl)quinoline **4b** or 4-(4-methoxystyryl)quinoline framework of **5b** resulted in 50% reduction in emission intensity of these complexes. Although it has been reported that the characteristic red shift of the photoluminescent spectra in the solid state are thought to be related to the formation of intermolecular aggregation [41], these results demonstrate the influence of introducing electron-withdrawing groups on phenyl ring for the effective lowering of the HOMO energy level as electron releasing group raises the HOMO energy level in Ir(III) complexes for their phosphorescence properties.

2.4. Electrochemical Studies

The electrochemical properties of the iridium metal complexes **4a–d** and **5a–d** in CHCl$_3$ solution were investigated by cyclic voltammetry (refer to Figures S1 and S2 in the Supplementary Materials) and square-wave voltammetry (Figures 11 and 12) using ferrocene/ferrocenium as the internal standard. All complexes show a similar profile with irreversible oxidation waves in the range 0.15–0.84 V and also undergo one electron reversible reduction profile (see Table S4 in the Supplementary Materials). The values of E$_{1/2}$ at 50 to 60 mV s^{-1} scan rates are listed in Table S4 in the Supplementary Materials. Previous studies of iridium complexes assigned these oxidation peaks to both the metal-centered Ir^{III}/Ir^{IV} oxidation process and the cyclometalated ligands [22,38,53–55]. The observed comparable oxidation potential values obtained for these complexes may be due to the same nature of the species involved in the process. In addition, upon switching on to cathodic sweep and electrode studied in the potential range +1.5 to −1.5 V and at a scan rate 50 mV s^{-1} (Table S4, Supplementary Materials), the voltammogram displays one reversible reduction peak with potentials range between −0.54 to −0.89 V, which were attributed to ligand-centered redox processes. Since all the complexes were differed only by nature of substituents and their positions either on the 2-phenyl- and/or 4-(4-phenylvinylene) rings, it is assumed that their HOMO and LUMO energy levels, and hence their redox potentials may be similar. Generally, compounds with electron withdrawing substituents were found to reduce more easily than those substituted with electron donating groups [56–58]. However, the reverse in reduction potentials was obtained for negative E$_{1/2}$ values of the complexes **4b** (at −0.64 V) with a combination of moderately resonance donating 4-fluorophenyl and 4-fluorostyryl groups and complex **5d** (at −0.62 V) with only strongly electron-donating 4-methoxyphenyl and 4-methoxystyryl groups. This may possibly explain the contributory nature of the electron-donating group to reduction processes. Moreover, higher negative E$_{1/2}$ values were obtained in complexes having a combination of an electron-donating and electron-withdrawing group on the same heterocyclic framework. Complex **4d** with a combination of 2-(4-methoxyphenyl) and 4-(4-fluorostyryl) groups was reduced at −0.82 V, whereas **5c** with a combination of 2-(4-chlorophenyl) and 4-(4-methoxystyryl) groups on the quinoline framework was reduced at −0.79 V. However, the reduction potentials in **4c** and **5c** at −0.54 V may further suggest that the electron acceptor performance of the ligand causes stabilization of the LUMO energy level of the complex [59]. In general, common trends observed in the electrochemistry are entirely closely related with those in the emission spectroscopy. It can reasonably, therefore, be confirmed that the oxidation potentials of these complexes primarily occur on the iridium metal centre, together with additional contributions from the cyclometalated quinoline framework. On the other hand, the reduction processes may be concentrated on the substituted styryl moiety of the quinoline chromophores.
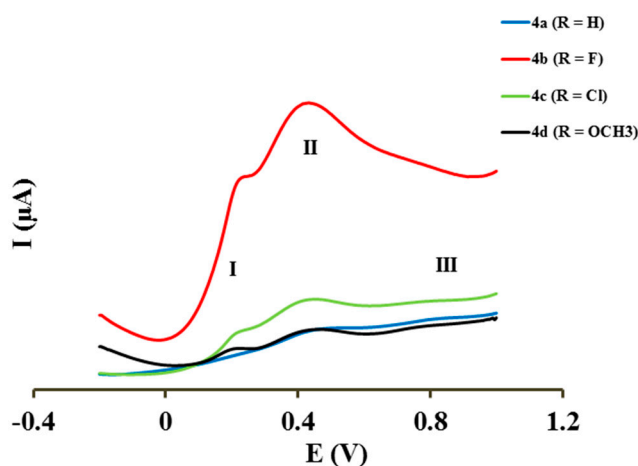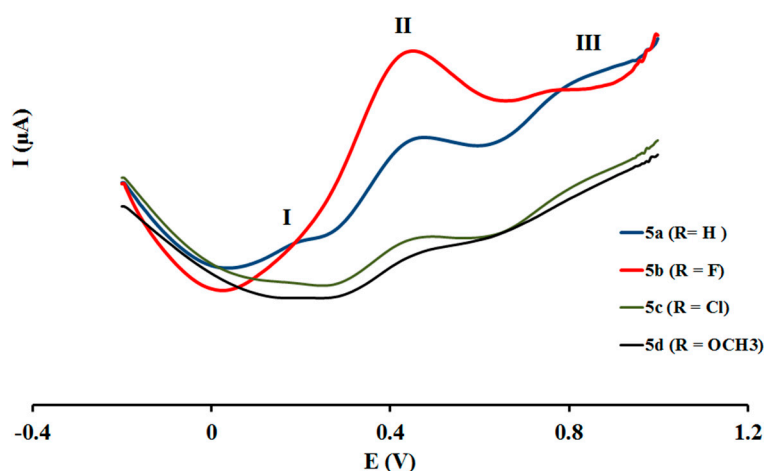
Figure 11. Square-wave voltammograms of (Ir(**4a**–**d**)$_3$) complexes.

Figure 12. Square-wave voltammograms of (Ir(**5a**–**d**)$_3$) complexes.

3. Materials and Methods

All chemical and reagents were analytically pure and used without further purification. Melting points were recorded on a Thermocouple digital melting point apparatus (Mettler Toledo LLC, Columbus, OH, USA) and are uncorrected. Microanalyses (C, H, and N) were carried out with a Fisons elemental analyzer (Fisons Thermo Scientific, Waltham, MA, USA) and Infrared spectra were recorded as powders using a Bruker VERTEX 70 FT-IR Spectrometer (Bruker Optics, Billerica, MA, USA) with a diamond ATR (attenuated total reflectance) accessory by using the thin-film method. The UV-Vis spectra were recorded on a Cecil CE 9500 (9000 Series) UV-Vis spectrometer (Cecil Instruments Cambridge, UK) while emission spectra were taken using a Perkin Elmer LS 45 fluorescence spectrometer (PerkinElmer, Llantrisant, UK) and Shimadzu RF-6000 Spectrofluoro-photometer (Shimadzu Europa GmbH, Duisburg, Germany). Quinine sulphate/1.0 N H$_2$SO$_4$ was used as a reference assuming a quantum yield of 0.55 with 360 nm excitation to determine luminescence quantum yields of the studied compounds, which was denoted as (Φf_x) with the following equation: $\Phi f_x = \Phi f_x (F_s A_x / F_x A_s)(n_s^2 / n_x^2)$, where the subscript x refers to the unknown sample and the subscript s to the standard, A is the absorbance at the excitation wavelength, F is the integrated emission across the band and n denotes the refractive index of the solvent [60]. For column chromatography, Merck Kieselgel 60 (0.063–0.200 mm) (Merck KGaA, Frankfurt, Germany) was used as stationary phase. NMR spectra were obtained as CDCl$_3$ solutions using Varian Mercury 300 MHz NMR spectrometer

(Varian Inc., Palo Alto, CA, USA) and the chemical shifts are quoted relative to the solvent peaks. Electrochemical experiment was performed using a PGSTAT 302 Autolab potentiostat (EcoChemie, Utrecht, The Netherlands) driven by the general purpose Electrochemical System data processing software (GPES, software version 4.9, Eco Chemie B.V, Kanaalweg, Utrecht, The Netherland). The electrochemical cell consists of a glassy carbon working electrode, platinum wire counter electrode and Ag/AgCl reference electrode. The oxidation and reduction measurements were recorded in a dichloromethane solution containing tetra(n-butyl)- ammonium tetrafluorophosphate as a supporting electrolyte at the scan rate of 50 mV s^{-1} under nitrogen conditions. Each oxidation potential was calibrated with the use of ferrocene/ferrocenium as a reference. The reported complexes were examined at a concentration of 10^{-3} M and supporting electrolyte at 10^{-1} M. The synthesis and analytical data of **1** have been described elsewhere [29].

3.1. Typical Procedure for the Suzuki–Miyaura Cross-Coupling of 1 with Arylboronic Acids

2-Aryl-4-chloroquinoline **1** (1 equiv.), 4-arylvinylboronic acid (1.2 equiv.), Pd(PPh$_3$)$_4$ (5% of 1), PCy$_3$ (10% of 1) and K$_2$CO$_3$ (2.0 equiv.) in 4:1 dioxane-water (15 mL/mmol of 1) were added to a two-necked flask equipped with a stirrer bar, rubber septum and a condenser. The mixture was flushed for 20 min with argon gas and a balloon filled with argon gas was connected to the top of the condenser. The mixture was heated with stirring at 80–90 °C under argon atmosphere for 3 h and then allowed to cool to room temperature. The cooled mixture was poured into ice-cold water and the product was taken-up into chloroform. The combined organic extracts were washed with brine, dried over anhydrous MgSO$_4$, filtered and then evaporated under reduced pressure. The residue was purified by column chromatography to afford **2**. The following products were prepared in this fashion:

4-(4-Fluorophenyvinyl)-2-phenylquinoline (**2a**). A mixture of **1a** (0.30 g, 1.25 mmol), 4-fluorophenyl vinylboronic acid (0.27 g, 1.63 mmol), Pd(PPh$_3$)$_4$ (0.07 g, 0.06 mmol), PCy$_3$ (0.04 g, 0.13 mmol) and K$_2$CO$_3$ (0.35 g, 2.51 mmol) in aqueous dioxane (15 mL) afforded **2a** as a yellow solid (0.16 g, 42%), mp. 128–130 °C; R$_f$ (chloroform) 0.52; ν_{max} (ATR) 481, 505, 672, 685, 754, 1228, 1508, 1578, 3056 cm^{-1}; δ_H (CDCl$_3$) 7.12 (t, 2H), 7.29 (d, *J* = 16.8 Hz, 1H), 7.48–7.59 (m, 6H), 7.70 (d, *J* = 16.8 Hz, 1H), 7.73 (d, *J* = 15 Hz, 1H), 7.99 (s, 1H), 8.13 (d, *J* = 7.5, 1H), 8.21 (d, *J* = 7.5 Hz, 3H); δ_C (75 MHz, CDCl$_3$) 114.9, 115.8 (d, $^2J_{CF}$ = 21.6 Hz), 123.0 (d, $^4J_{CF}$ = 2.3 Hz), 123.1, 125.3, 126.2, 127.5, 128.6 (d, $^3J_{CF}$ = 8.3 Hz), 128.8, 129.2, 129.5, 130.3, 132.7 (d, $^4J_{CF}$ = 3.4 Hz), 133.5, 139.7, 143.3, 148.7, 157.1, 162.9 (d, $^1J_{CF}$ = 247.4 Hz); Anal. Calcd. for C$_{23}$H$_{16}$NF: C, 84.89; H, 4.96; N, 4.31. Found: C, 84.94; H, 4.92; N, 4.38.

2-(4-Fluorophenyl)-4-(4-fluorophenyvinyl)quinoline (**2b**). A mixture of **1b** (0.30 g, 1.16 mmol), 4-fluorophenylvinylboronic acid (0.25 g, 1.51 mmol), Pd(PPh$_3$)$_4$ (0.07 g, 0.06 mmol), PCy$_3$ (0.03 g, 0.12 mmol) and K$_2$CO$_3$ (0.32 g, 2.32 mmol) in aqueous dioxane (15 mL) afforded **2b** as a yellow solid (0.15 g, 38%), mp. 125–126 °C; Rf (chloroform) 0.72; ν_{max} (ATR) 481, 505, 629, 754, 837, 956, 1155, 1225, 1424, 1501, 1579, 3055, 2922 cm^{-1}; δH (CDCl$_3$): 7.13–7.22 (m, 4H), 7.34 (d, *J* = 15.3 Hz, 1H), 7.54–7.64 (m, 3H), 7.74 (d, *J* = 16.8 Hz, 1H), 7.76 (d, *J* = 16.8 Hz, 1H), 7.98 (s, 1H), 8.16–8.22 (m, 4H); δ_C (75 MHz, CDCl$_3$) 114.7, 115.6, 115.7 (d, $^2J_{CF}$ = 21.3 Hz), 115.8, 116.1, 118.4, 123.1 (d, $^4J_{CF}$ = 2.6 Hz), 123.3, 124.5, 125.3, 126.3, 128.8 (d, $^3J_{CF}$ = 8.0 Hz), 129.4 (d, $^3J_{CF}$ = 8.6 Hz), 129.7, 130.3, 132.7, 132.8, 133.8, 135.9, 143.6, 148.7, 156.1, 161.7 (d, $^1J_{CF}$ = 59.2 Hz), 165.0 (d, $^1J_{CF}$ = 58.6 Hz); Anal. Calcd. for C$_{23}$H$_{15}$NF$_2$: C, 80.44; H, 4.41; N, 4.08. Found: C, 80.70; H, 4.78; N, 4.25.

2-(4-Chlorophenyl)-4-(4-fluorophenyvinyl)quinoline (**2c**). A mixture of **1c** (0.09 g, 0.35 mmol), 4-fluorophenylvinylboronic acid (0.08 g, 0.46 mmol), Pd(PPh$_3$)$_4$ (0.02 g, 0.02 mmol), PCy$_3$ (0.01 g, 0.04 mmol) and K$_2$CO$_3$ (0.09 g, 0.70 mmol) in aqueous dioxane (15 mL) afforded **2c** as off-white solid (0.15 g, 48%), mp. 98–101°C; R$_f$ (chloroform) 0.43; ν_{max} (ATR) 459, 533, 689, 753, 826, 836, 1090, 1321, 1416, 1486, 1543, 1572, 1588, 2924 cm^{-1}; δ_H (CDCl$_3$) 7.01 (t, 1H), 7.36–7.41 (m, 1H), 7.49 (d, *J* = 9.0 Hz, 3H), 7.63 (t, 1H), 7.78 (t, 2H), 7.99 (s, 1H), 8.09 (d, *J* = 9.3 Hz, 3H), 8.15 (d, *J* = 7.5 Hz, 2H), 8.22 (d, *J* = 9.3 Hz, 1H); δ_C (75 MHz, CDCl$_3$) 115.6 (d, $^2J_{CF}$ = 21.6 Hz), 118.7, 123.9, 125.3, 127.5, 127.8 (d, $^3J_{CF}$ = 7.7 Hz), 128.7, 129.1,

130.0, 130.8, 131.5, 133.4 (d, $^4J_{CF}$ = 3.4 Hz), 136.1, 136.9, 143.4, 148.9, 155.9, 162.3 (d, $^1J_{CF}$ = 245.9 Hz); Anal. Calcd. for $C_{23}H_{15}NFCl$: C, 76.86; H, 4.21; N, 3.90. Found: C, 76.42; H, 4.54; N, 3.55.

4-(4-Fluorophenyvinyl)-2-(4-methoxyphenyl)quinoline (**2d**). A mixture of **1d** (0.30 g, 1.11 mmol), 4-fluorophenylvinylboronic acid (0.24 g, 1.44 mmol), Pd(PPh$_3$)$_4$ (0.07 g, 0.06 mmol), PCy$_3$ (0.03 g, 0.11 mmol) and K$_2$CO$_3$ (0.31 g, 2.22 mmol) in aqueous dioxane (15 mL) afforded **2d** as a brilliant yellow solid (0.19 g, 48%), mp. 125–128 °C; R_f (chloroform) 0.50; ν_{max} (ATR) 481, 753, 838, 1091, 1173, 1229, 1416, 1486, 1503, 1543, 1586, 2927, 3045 cm^{-1}; δ_H (CDCl$_3$) 3.88 (s, 3H), 6.96 (m, 1H), 7.04–7.15 (m, 3H), 7.32 (d, *J* = 16.8 Hz, 1H), 7.52 (t, 1H), 7.58–7.62 (m, 2H), 7.71 (d, *J* = 15.3 Hz, 1H), 7.73 (d, *J* = 16.8 Hz, 1H), 7.97 (s, 1H), 8.12–8.18 (m, 3H); δ_C (75 MHz, CDCl$_3$) 55.4, 114.2, 114.7, 115.9 (d, $^2J_{CF}$ = 21.6 Hz), 118.3, 123.2, 123.3 (d, $^4J_{CF}$ = 2.3 Hz), 124.4, 125.1, 125.9, 128.7 (d, $^3J_{CF}$ = 8.0 Hz), 128.8, 129.5, 129.7, 130.2, 130.7 (d, $^3J_{CF}$ = 8.0 Hz), 132.3, 132.8 (d, $^4J_{CF}$ = 3.4 Hz), 133.5, 143.3, 148.7, 156.7, 160.8, 162.9 (d, $^1J_{CF}$ = 247.4 Hz); Anal. Calcd. for $C_{24}H_{18}NFO$: C, 81.10; H, 5.11; N, 3.94. Found: C, 81.43; H, 5.39; N, 4.12.

4-(4-Methoxyphenyvinyl)-2-phenylquinoline (**3a**). A mixture of **1a** (0.30 g, 1.25 mmol), 4-methoxyphenylvinylboronic acid (0.27 g, 1.50 mmol), Pd(PPh$_3$)$_4$ (0.07 g, 0.06 mmol), PCy$_3$ (0.04 g, 0.12 mmol) and K$_2$CO$_3$ (0.35 g, 2.51 mmol) in aqueous dioxane (15 mL) afforded **3a** as a yellow oil (0.20 g, 67%); R_f (chloroform) 0.44; ν_{max} (ATR) 515, 691, 754, 767, 1028, 1172, 1250, 1508, 1583, 1604, 2834, 2930 cm^{-1}; δ_H (CDCl$_3$) 3.86 (s, 3H), 6.97 (d, *J* = 9.0 Hz, 2H), 7.36 (d, *J* = 15.9 Hz, 1H), 7.49–7.61 (m, 6H), 7.71 (d, *J* = 15.3 Hz, 1H), 7.74 (d, *J* = 15.2 Hz, 1H), 8.04 (s, 1H), 8.18–8.23 (m, 4H); δ_C (75 MHz, CDCl$_3$) 55.3, 113.7, 114.3, 114.7, 118.8, 120.9, 123.3, 123.7, 124.7, 125.4, 126.1, 126.2, 127.4, 127.5, 128.5, 128.7, 128.8, 129.2, 129.3, 129.4, 129.7, 130.1, 130.2, 130.4, 133.6, 134.5, 139.8, 143.9, 148.7, 157.1, 160.1; Anal. Calcd. for $C_{24}H_{19}NO$: C, 85.42; H, 5.68; N, 4.15. Found: C, 85.77; H, 5.85; N, 4.34.

2-(4-Fluorophenyl)-4-(4-methoxyphenylvinyl)quinoline (**3b**). A mixture of **1b** (0.30 g, 1.16 mmol), 4-methoxyphenylvinylboronic acid (0.25 g, 1.39 mmol), Pd(PPh$_3$)$_4$ (0.07 g, 0.06 mmol), PCy$_3$ (0.03 g, 0.12 mmol) and K$_2$CO$_3$ (0.32 g, 2.32 mmol) in aqueous dioxane (15 mL) afforded 3b as a light yellow solid (0.09 g, 42%), mp. 95–98 °C; R_f (chloroform) 0.67; ν_{max} (ATR) 755, 839, 964, 1156, 1172, 1250, 1416, 1486, 1503, 1544, 1582, 2958 cm^{-1}; δ_H (CDCl$_3$) 3.87 (s, 3H), 6.97 (d, *J* = 8.1 Hz, 2H), 7.22 (t, 3H), 7.36 (d, *J* = 15.9 Hz, 1H), 7.57 (m, 4H), 7.71 (d, *J* = 15.3 Hz, 1H), 7.99 (s, 1H), 8.15–8.21 (m, 3H); δ_C (75 MHz, CDCl$_3$) 55.4, 113.7, 114.1, 114.3, 114.4, 115.6 (d, $^4J_{CF}$ = 5.1 Hz), 115.9 (d, $^4J_{CF}$ = 5.2 Hz), 118.5, 120.9, 123.5 (d, $^2J_{CF}$ = 22.8 Hz), 124.7, 126.2, 126.3, 128.5, 129.3, 129.4 (d, $^3J_{CF}$ = 8.0 Hz), 129.6, 129.8, 130.2, 130.1, 130.2, 130.4, 133.8, 134.6, 160.2 (d, $^1J_{CF}$ = 247.4 Hz); Anal. Calcd. for $C_{24}H_{18}NOF$: C, 81.10; H, 5.11; N, 3.94. Found: C, 81.40; H, 5.36; N, 4.16.

2-(4-Chlorophenyl)-4-(4-methoxyphenylvinyl)quinoline (**3c**). A mixture of **1c** (0.25 g, 0.91 mmol), 4-methoxyphenylvinylboronic acid (0.20 g, 1.09 mmol), Pd(PPh$_3$)$_4$ (0.05 g, 0.05 mmol), PCy$_3$ (0.03 g, 0.09 mmol) and K$_2$CO$_3$ (0.25 g, 1.82 mmol) in aqueous dioxane (15 mL) afforded **3c** as a bright yellow solid (0.11 g, 41%), mp. 144–146 °C; R_f (chloroform) 0.70; ν_{max} (ATR) 518, 529, 763, 822, 835, 966, 1027, 1172, 1253, 1509, 1582 cm^{-1}; δ_H (CDCl$_3$) 3.87 (s, 3H), 6.96 (d, *J* = 8.4 Hz, 2H), 7.35 (d, *J* = 15.9 Hz, 1H), 7.51 (d, *J* = 8.4 Hz, 2H), 7.58–7.70 (m, 4H), 7.70 (d, *J* = 16.4 Hz, 2H), 7.99 (s, 1H), 8.14–8.20 (m, 3H); δ_C (75 MHz, CDCl$_3$) 55.4, 114.3, 120.8, 123.3, 125.4, 126.3, 127.4, 128.5, 128.8, 128.9, 129.3, 129.6, 130.3, 133.8, 134.6, 135.4, 138.3, 144.1, 148.7, 155.8, 160.2; Anal. Calcd. for $C_{24}H_{18}NOCl$: C, 77.61; H, 4.89; N, 3.77. Found: C, 78.02; H, 4.76; N, 3.58

2-(4-Methoxyphenyl)-4-(4-methoxyphenylvinyl)quinoline (**3d**). A mixture of **1d** (0.30 g, 1.11 mmol), 4-methoxyphenylvinylboronic acid (0.24 g, 1.33 mmol), Pd(PPh$_3$)$_4$ (0.07 g, 0.06 mmol), PCy$_3$ (0.03 g, 0.11 mmol) and K$_2$CO$_3$ (0.31 g, 2.22 mmol) in aqueous dioxane (15 mL) afforded **3d** as a cream-white solid (0.19 g, 47%), mp. 75–78 °C; R_f (chloroform) 0.22; ν_{max} (ATR) 533, 751, 823, 1026, 1171, 1250, 1326, 1491, 1574, 2922 cm^{-1}; δ_H (CDCl$_3$) 3.88 (s, 6H), 7.04 (d, *J* = 9.3 Hz, 3H), 7.58 (t, 2H), 7.75 (t, 2H), 7.92 (s, 1H), 8.11 (d, *J* = 7.8 Hz, 2H), 8.18 (t, 5H); δ_C (75 MHz, CDCl$_3$) 55.4, 114.1, 114.3, 118.6, 123.9, 124.9, 126.8,

127.4, 127.5, 128.8, 129.8, 130.4, 131.0, 131.2, 142.9, 149.0, 156.8, 161.1; Anal. Calcd. for $C_{25}H_{21}NO_2$: C, 81.71; H, 5.76; N, 3.81. Found: C, 82.05; H, 5.98; N, 3.89.

3.2. Synthetic Method and Characterization of Iridium(III) Complexes **4a–d** and **5a–d**

The reported cyclometalated Ir(III) complexes **4a–d**) and **5a–d** were synthesized by a slight modification to the method as previously reported in the literature [35]. In a 2-necked round bottomed flask, each of the ligand **2a–d** or **3a–d** (1 equiv.) was dissolved in 3:1 2-ethoxyethanol–water (*v/v*), and the mixture was purged with argon gas for 5 min, before iridium trichloride hydrate $[IrCl_3(H_2O)_3]$ (one-third equimolar ratio of ligand) was added and the mixture heated at 120 °C under argon atmosphere for 12 h. After reaction, the solution was allowed to cool to room temperature and then filtered. The filtrate was concentrated under vacuum to remove 2-ethoxyethanol, and the crude complex product was further purified by column chromatography in ethyl acetate-toluene (9:1) to obtain brown powder. The iridium complexes were characterized by ^{1}H NMR and elemental analysis. The ^{1}H NMR peaks of the complexes are very similar to those of the starting ligands due to chemical equivalence. The principal difference is the downfield shift due to the loss of one hydrogen atom and coordination of the N^C-ligand to the iridium metal center.

Complex **4a**: Brown solid (54 mg, 27%), ^{1}H NMR (300 MHz, CDCl₃): δ 6.91 (t), 7.02 (d, *J* = 7.5 Hz), 7.07 (d, *J* = 7.5 Hz), 7.12 (s), 7.19 (t), 7.28 (d, *J* = 7.8 Hz), 7.38 (d, *J* = 7.5 Hz), 7.44 (d, *J* = 6.0 Hz), 7.54–7.99 (m), 8.05 (d, *J* = 3.3 Hz), 8.28 (d, *J* = 7.8), 8.50 (d, *J* = 7.5 Hz). Anal. Calcd. for $IrC_{69}H_{45}N_3F_3$: C, 71.12; H, 3.89; N, 3.61. Found: C, 71.45; H, 3.96; N, 3.87.

Complex **4b**: Brown solid (62 mg, 30%), ^{1}H NMR (300 MHz, CDCl₃): δ 6.98 (s), 7.11 (s), 7.14–7.23 (m), 7.44 (d, *J* = 15.3 Hz), 7.07 (d, *J* = 7.5 Hz), 7.12 (s), 7.19 (t), 7.28 (d, *J* = 7.8 Hz), 7.38 (d, *J* = 7.5 Hz), 7.44 (d, *J* = 6.0 Hz), 7.54–7.67 (m), 7.73 (s), 7.77–7.81 (m), 8.00 (s), 8.20 (d, *J* = 7.5 Hz), 8.40 (s, br). Anal. Calcd. for $IrC_{69}H_{42}N_3F_6$: C, 67.97; H, 3.47; N, 3.45. Found: C, 67.83; H, 3.56; N, 3.54.

Complex **4c**: Pink solid. Yield: 25% (31 mg), ^{1}H NMR (300 MHz, CDCl₃): δ 6.61 (d, *J* = 12.3 Hz), 6.81 (d, *J* = 3.0 Hz), 6.86 (d, *J* = 3.0 Hz), 6.99–7.07 (m), 7.37–7.41 (m), 7.50 (d, *J* = 6.0 Hz), 7.64 (t), 7.80 (t), 7.94 (s), 8.11 (d, *J* = 7.8 Hz), 8.22 (t). Anal. Calcd. for $IrC_{69}H_{42}N_3F_3Cl_3$: C, 65.32; H, 3.34; N, 3.31. Found: C, 65.53; H, 3.48; N, 3.47.

Complex **4d**: Dark brown solid (30 mg, 28%), ^{1}H NMR (300 MHz, CDCl₃): δ 3.65 (s, OCH₃), 6.80 (d, *J* = 7.8 Hz), 6.97 (d, *J* = 7.8 Hz), 7.09 (t), 7.17 (d, *J* = 7.8 Hz), 7.52–7.68 (m), 7.73–7.79 (m), 7.84 (d, *J* = 9.0 Hz), 7.96 (d, *J* = 7.5 Hz), 8.00 (s), 8.13 (d, *J* = 9.3 Hz), 8.24 (d, *J* = 9.3 Hz), 8.41 (br, s), 8.64 (s). Anal. Calcd. for $IrC_{72}H_{51}N_3F_3O_3$: C, 72.16; H, 4.29; N, 3.51. Found: C, 72.42; H, 4.27; N, 3.66.

Complex **5a**: Brown solid (74 mg, 53%), ^{1}H NMR (300 MHz, CDCl₃): δ 3.94 (s, OCH₃), 7.16 (d, *J* = 9.3 Hz), 7.30 (t), 7.43 (t), 7.62 (d, *J* = 9.3 Hz), 7.71 (m), 7.87 (s), 7.93 (d, *J* = 9.3 Hz), 8.14 (d, *J* = 7.5 Hz), 8.34 (br, s). Anal. Calcd. for $IrC_{72}H_{54}N_3O_3$: C, 71.98; H, 4.53; N, 3.50. Found: C, 71.85; H, 4.33; N, 3.57.

Complex **5b**: Brown solid (79 mg, 57%), ^{1}H NMR (300 MHz, CDCl₃): δ 3.74 (s, OCH₃), 6.93 (d, *J* = 7.8 Hz), 7.60 (d, *J* = 3.0 Hz), 7.61 (d, *J* = 13.5 Hz), 7.67 (d, *J* = 7.5 Hz), 7.80 (s), 7.95 (d, *J* = 7.5 Hz), 8.02 (d, *J* = 7.5 Hz), 8.53 (br, s). Anal. Calcd. for $IrC_{72}H_{51}N_3F_3O_3$: C, 68.88; H, 4.09; N, 3.35. Found: C, 68.62; H, 4.37; N, 3.53.

Complex **5c**: Brown solid (74 mg, 42%), ^{1}H NMR (300 MHz, CDCl₃): δ 3.96 (s, OCH₃), 7.14 (d, *J* = 8.7 Hz), 7.56 (d, *J* = 8.7 Hz), 7.52 (d, *J* = 8.7 Hz), 7.77–7.80 (br, s), 8.02 (d, *J* = 8.1 Hz), 8.16 (d, *J* = 8.4 Hz), 8.31 (d, *J* = 8.4 Hz). Anal. Calcd. for $IrC_{72}H_{51}N_3Cl_3O_3$: C, 66.28; H, 3.94; N, 3.22. Found: C, 66.12; H, 3.80; N, 3.54.

Complex **5d**: Dark brown solid (85 mg, 45%), ^{1}H NMR (300 MHz, CDCl$_3$): δ 3.68 (s, OCH$_3$), 3.91 (s, OCH$_3$), 6.88 (d, *J* = 7.8 Hz), 7.11 (d, *J* = 9.3 Hz), 7.56 (d, *J* = 7.5 Hz), 7.61 (s), 7.76 (s), 7.82 (t), 8.04 (t), 8.46 (d, *J* = 9.0 Hz). Anal. Calcd. for IrC$_{75}$H$_{60}$N$_3$O$_6$: C, 69.75; H, 4.68; N, 3.25. Found: C, 69.52; H, 4.87; N, 3.64.

3.3. DFT Computation

The ligand (**2a**) and its corresponding iridium(III) complex (**4a**) were optimised in the gas phase using the DFT method. The B3LYP functional was used in conjunction with the 6-31G(d,p) basis set for all atoms except for iridium, where the LANL2DZ ECP basis set was used. The ligand was also optimised in three solvents, namely methanol, chloroform and dimethyl formamide. The complex was optimised in methanol. Solvent computations were based on the PCM model [61,62]. Frequency computations were performed on all of the optimised structures to confirm the nature of the stationary points. All the structures were optimised as ground states without any imaginary frequency. To simulate the UV-Vis spectra, Time-dependent density functional theory (TDDFT) computations were performed for the ligand in chloroform and the complex in methanol. All computations were carried out using Gaussian 09 software running on Gridchem [63–65].

4. Conclusions

This study has shown that the electronic absorption, emission and electrochemical properties of the complexes originate from the ligands and the both electron-donating and electron-withdrawing groups on the quinoline framework play an important role in the determination of the optical properties, the quantum yields and the redox properties. It has been shown among the d$_6$ metals, that the cyclometalated iridium(III) complexes represent the most promising high performance emitters due to their strong Ir-C bonds, which ensure good photo- and thermal stability, thermally accessible destabilization and non-emissive metal centred (MC) states. The molecular framework of the quinoline ligands used in this study is linked directly to the aryl ring or through a pi-conjugated bridge leading to low redox potentials and a greater tendency to undergo electron transfer reactions. It is quite interesting to observe the tunable photoluminescence from blue to green to red for the iridium(III) complexes on the basis of π→π* elongation of conjugation, electron-withdrawing or electron-donating substituent at the 4-position of the phenylvinylene moiety of the quinoline framework. The reported Ir(III) complexes may find use as potential emissive dopants, fluorescent marker, electron transport materials for OLEDs application, and drug discovery.

Author Contributions: A.O.A. and A.S.A. collaborated in the experimental work with M.J.M. as a postdoctoral mentor of A.O.A., L.R. and P.R. performed DFT studies and helped with the discussion of the corresponding data. All of the authors contributed to the compilation of the manuscript with A.O.A. as the lead author.

Conflicts of Interest: The authors declare no conflict of interest.

References

1.　Welter, S.; Brunner, K.; Hofstraat, J.W.; De Cola, L. Electroluminescent device with reversible switching between red and green emission. *Nature* **2003**, *421*, 54–57. [CrossRef] [PubMed]

2.　Yang, C.H.; Beltran, J.; Lemaur, V.; Cornil, J.; Hartmann, D.; Sarfert, W.; Frohlich, R.; Bizzarri, C.; De Cola, L. Iridium metal complexes containing *N*-heterocyclic carbene ligands for blue-light-emitting electrochemical cells. *Inorg. Chem.* **2010**, *49*, 9891–9901. [CrossRef] [PubMed]

3.　Slinker, J.D.; Gorodetsky, A.A.; Lowry, M.S.; Wang, J.J.; Parker, S.; Rohl, R.; Bernhard, S.; Malliarasa, G.G. Efficient yellow electroluminescence from a single layer of a cyclometalated iridium complex. *J. Am. Chem. Soc.* **2004**, *126*, 2763–2767. [CrossRef] [PubMed]

4.　Bolink, H.J.; Coronado, E.; Costa, R.D.; Lardies, N.; Orti, E. Near-quantitative internal quantum efficiency in a light-emitting electrochemical cell. *Inorg. Chem.* **2008**, *47*, 9149–9151. [CrossRef] [PubMed]

5.　Bolink, H.J.; Cappelli, L.; Coronado, E.; Gratzel, M.; Orti, E.; Costa, R.D.; Viruela, P.M.; Nazeeruddin, M.K. Stable single-layer light-emitting electrochemical cell using 4,7-Diphenyl-1,10-phenanthroline-bis(2-phenylpyridine)iridium(III) hexafluorophosphate. *J. Am. Chem. Soc.* **2006**, *128*, 14786–14787. [CrossRef] [PubMed]

6.　Su, H.-C.; Fang, F.-C.; Hwu, T.-Y.; Hsieh, H.-H.; Chen, H.-F.; Lee, G.-H.; Peng, S.-M.; Wong, K.-T.; Wu, C.-C. Highly efficient orange and green solid-state light-emitting electrochemical cells based on cationic Ir[III] complexes with enhanced steric hindrance. *Adv. Funct. Mater.* **2007**, *17*, 1019–1027. [CrossRef]

7.　Colman, E.Z.; Slinker, J.D.; Parker, J.B.; Malliaras, G.G.; Bernhard, S. Improved turn-on times of light-emitting electrochemical cells. *Chem. Mater.* **2008**, *20*, 388–396. [CrossRef]

8.　Dixon, I.M.; Collin, J.P.; Sauvage, J.P.; Flamigni, L.; Encinas, S.; Barigelletti, F. A family of luminescent coordination compounds: Iridium(III) polyimine complexes. *Chem. Soc. Rev.* **2000**, *29*, 385–391. [CrossRef]

9.　Ulbricht, C.; Beyer, B.; Friebe, C.; Winter, A.; Schubert, U.S. Recent developments in the application of phosphorescent iridium(III) complex systems. *Adv. Mater.* **2009**, *21*, 4418–4441. [CrossRef]

10.　Chi, Y.; Chou, R.-T. Transition-metal phosphors with cyclometalating ligands: Fundamentals and applications. *Chem. Soc. Rev.* **2010**, *39*, 638–655. [CrossRef] [PubMed]

11.　Haugland, R.P. *The Handbook—A Guide to Fluorescent Probes and Labelling Technologies*, 10th ed.; Molecular Probes Inc.: Eugene, OR, USA, 2005.

12.　Lo, K.K.-W.; Li, S.P.-Y.; Zhang, K.Y. Development of luminescent iridium(III) polypyridine complexes as chemical and biological probes. *New J. Chem.* **2011**, *35*, 265–287. [CrossRef]

13.　Fernandez-Moreira, V.; Thorp-Greenwood, F.L.; Coogan, M.P. Application of d_6 transition metal complexes in fluorescence cell imaging. *Chem. Commun.* **2010**, *46*, 186–202. [CrossRef] [PubMed]

14.　Margapoti, E.; Shukla, V.; Valore, A.; Sharma, A.; Dragonetti, C.; Kitts, C.C.; Roberto, D.; Murgia, M.; Ugo, R.; Muccini, M. Excimer emission in single layer electroluminescent devices based on [Ir(4,5-diphenyl-2-methylthiazolo)$_2$(5-methyl-1,10-phenanthroline)]$^+$[PF$_6$]$^-$. *J. Phys. Chem. C* **2009**, *113*, 12517–12522. [CrossRef]

15.　Margapoti, E.; Muccini, M.; Sharma, A.; Colombo, A.; Dragonetti, C.; Robertob, D.; Valore, A. Optoelectronic properties of OLEC devices based on phenylquinoline and phenylpyridine ionic iridium complexes. *Dalton Trans.* **2012**, *41*, 9227–9231. [CrossRef] [PubMed]

16.　Shen, Y.; Kuddes, D.D.; Naquin, C.A.; Hesterberg, T.W.; Kusmierz, C.; Holliday, B.J.; Slinker, J.D. Improving light-emitting electrochemical cells with ionic additives. *Appl. Phys. Lett.* **2013**, *102*, 203305–203309. [CrossRef]

17.　Meier, S.B.; Hartmann, D.; Tordera, D.; Bolink, H.J.; Winnackera, A.; Sarfert, W. Dynamic doping and degradation in sandwich-type light-emitting electrochemical cells. *Phys. Chem. Chem. Phys.* **2012**, *14*, 10886–10890. [CrossRef] [PubMed]

18.　Zaarour, M.; Guerchais, V.; Le Bozec, H.; Dragonetti, C.; Righetto, S.; Roberto, D.; De Angelis, F.; Fantacci, S.; Lobello, M.G. An investigation on the second order nonlinear optical response of tris-cyclometallated Ir(III) complexes with various substituted 2-phenylpyridines. *Dalton Trans.* **2013**, *42*, 155–159. [CrossRef] [PubMed]

19.　Zaarour, M.; Singh, A.; Latouche, C.; William, J.G.; Ledoux-Rak, I.; Zyss, J.; Boucekkine, A.; Le Bozec, H.; Guerchais, V.; Dragonetti, C.; et al. Linear and nonlinear optical properties of tris cyclometalated phenylpyridine Ir(III) complexes incorporating π-conjugated substituents. *Inorg. Chem.* **2013**, *52*, 7987–7994. [CrossRef] [PubMed]

20. Albini, A.; Fasani, E. A specialist periodical report. *Photochemistry* **2016**, *43*, 148–172.

21. Tsuboyama, A.; Iwawaki, H.; Furugori, M.; Mukaide, T.; Kamatani, J.; Igawa, S.; Moriyama, T.; Miura, S.; Takiguchi, T.; Okada, S.; et al. Homoleptic cyclometalated iridium complexes with highly efficient red phosphorescence and application to organic light-emitting diode. *J. Am. Chem. Soc.* **2003**, *125*, 12971–12979. [CrossRef] [PubMed]

22. Wu, F.-I.; Su, H.-J.; Shu, C.-F.; Luo, L.; Diau, W.-G.; Cheng, C.-H.; Duan, J.-P.; Lee, G.-H. Tuning the emission and morphology of cyclometalated iridium complexes and their applications to organic light-emitting diodes. *J. Mater. Chem.* **2005**, *15*, 1035–1042. [CrossRef]

23. Park, Y.H.; Park, G.Y.; Kim, Y.S. Heteroleptic iridium(III) complexes with phenylpridine and diphenylquinoline derivative ligands. *Mol. Cryst. Liq. Cryst.* **2007**, *462*, 197–207. [CrossRef]

24. Dahule, H.K.; Dhoble, S.J. Effect of substituents on the photoluminescence performance of Ir(III) complexes: Synthesis and photo physical properties. *J. Chem. Biol. Phys. Sci.* **2012**, *2*, 1539–1550.

25. Lupton, J.M.; Samuel, I.D.W.; Frampton, M.J.; Beavington, R.; Burn, P.L. Control of electrophosphorescence in conjugated dendrimer light-emitting diodes. *Adv. Funct. Mater.* **2001**, *11*, 287–294. [CrossRef]

26. Lo, S.-C.; Richards, G.J.; Markham, J.P.J.; Namdas, E.B.; Sharma, S.; Burn, P.L. A light-blue phosphorescent dendrimer for efficient solution-processed light-emitting diodes. *Adv. Funct. Mater.* **2005**, *15*, 1451–1458. [CrossRef]

27. Li, X.; Chen, Z.; Zhao, Q.; Shen, L.; Li, F.; Yi, T.; Cao, Y.; Huang, C. Nonconjugated dendritic iridium(III) complexes with tunable pyridine-based ligands: Synthesis, photophysical, electrochemical, and electroluminescent properties. *Inorg. Chem.* **2007**, *46*, 5518–5527. [CrossRef] [PubMed]

28. Lowry, M.S.; Bernhard, S. Synthetically tailored excited states: Phosphorescent, cyclometalated iridium(III) complexes and their applications. *Chem. Eur. J.* **2006**, *12*, 7970–7977. [CrossRef] [PubMed]

29. Adeloye, A.O.; Mphahlele, M.J. 2,4-Diarylquinolines: Synthesis, absorption and emission properties. *J. Chem. Res.* **2014**, *38*, 254–259. [CrossRef]

30. Aranda, B.S.; Aguirre, P.; Moya, S.A.; Bonneau, M.; Williams, J.G.; Toupet, L.; Escadeillas, M.; Le Bozec, H.; Guerhais, V. Luminescent bis-cyclometallated iridium(III) complexes containing phosphine-based ligands: Influence of the PˆN bridge. *Polyhedron* **2015**, *86*, 120–124. [CrossRef]

31. Grushin, V.V.; Herron, N.; LeCloux, D.D.; Marshall, W.J.; Petrov, V.A.; Wang, Y. New, efficient electroluminescent materials based on organometallic Ir complexes. *Chem. Commun.* **2001**, *16*, 1494–1495. [CrossRef]

32. Jung, S.O.; Kang, Y.; Kim, H.S.; Kim, Y.H.; Lee, C.L.; Kim, J.J.; Lee, S.K.; Kwon, S.K. Effect of substitution of methyl groups on the luminescence performance of Ir[III] complexes: Preparation, structures, electrochemistry, photophysical properties and their applications in organic light-emitting diodes (OLEDs). *Eur. J. Inorg. Chem.* **2004**, *16*, 3415–3423. [CrossRef]

33. Lee, S.J.; Park, K.M.; Yang, K.; Kang, Y. Blue phosphorescent Ir(III) complex with high color purity: *fac*-Tris(2′,6′-difluoro-2,3′-bipyridinato-N,C$^{4'}$)iridium(III). *Inorg. Chem.* **2009**, *48*, 1030–1037. [CrossRef] [PubMed]

34. Lowry, M.S.; Hudson, W.R.; Pascal, R.A., Jr.; Bernhard, S. Accelerated luminophore discovery through combinatorial synthesis. *J. Am. Chem. Soc.* **2004**, *126*, 14129–14135. [CrossRef] [PubMed]

35. Lowry, M.S.; Goldsmith, J.I.; Slinker, J.D.; Rohl, R.; Pascal, R.A., Jr.; Malliaras, G.G.; Bernhard, S. Single-layer electroluminescent devices and photoinduced hydrogen production from an ionic iridium(III) complex. *Chem. Mater.* **2005**, *17*, 5712–5719. [CrossRef]

36. Laskar, I.R.; Chen, T.M. Tuning of wavelengths: Synthesis and photophysical studies of iridium complexes and their applications in organic light emitting devices. *Chem. Mater.* **2004**, *16*, 111–117. [CrossRef]

37. Coppo, P.; Plummer, E.A.; De Cola, L. Tuning iridium(III) phenylpyridine complexes in the "almost blue" region. *Chem. Commun.* **2004**, *15*, 1774–1775. [CrossRef] [PubMed]

38. Sengottuvelan, N.; Seo, H.-J.; Kang, S.K.; Kim, Y.-I. Tuning photophysical and electrochemical properties of heteroleptic cationic iridium(III) complexes containing substituted 2-phenylquinoxaline and biimidazole. *Bull. Korean Chem. Soc.* **2010**, *31*, 2309–2314. [CrossRef]

39. Lamansky, S.; Djurovich, P.; Murphy, D.; Abdel-Razzaq, F.; Kwong, R.; Tsyba, I.; Bortz, M.; Mui, B.; Bau, R.; Thompson, M.E. Synthesis and characterization of phosphorescent cyclometalated iridium complexes. *Inorg. Chem.* **2001**, *40*, 1704–1711. [CrossRef] [PubMed]

40. Colombo, M.G.; Brunold, T.C.; Riedener, T.; Gudel, H.U.; Fortsch, M.; Burgi, H. Facial *tris* cyclometalated rhodium(3+) and iridium(3+) complexes: Their synthesis, structure, and optical spectroscopic properties. *Inorg. Chem.* **1994**, *33*, 545–550. [CrossRef]

41. Park, J.; Park, J.S.; Park, Y.G.; Lee, J.Y.; Kang, J.W.; Liu, J.; Dai, L.; Jin, S.H. Synthesis, characterization of the phenylquinoline-based on iridium(III) complexes for solution processable phosphorescent organic light-emitting diodes. *Org. Electron.* **2013**, *14*, 2114–2123. [CrossRef]

42. Joshi, N.B.; Gangola, P.; Pant, D.D. Internal heavy atom effect on the radiative and non-radiative rate constants in xanthene dyes. *J. Lumin.* **1979**, *21*, 111–118. [CrossRef]

43. Duprez, V.; Biancardo, M.; Spanggaard, H.; Krebs, F.C. Synthesis of conjugated polymers containing terpyridine–ruthenium complexes: Photovoltaic applications. *Macromolecules* **2005**, *38*, 10436–10448. [CrossRef]

44. Schmid, B.; Graces, F.O.; Watts, R.J. Synthesis and characterizations of cyclometalated iridium(III) solvento complexes. *Inorg. Chem.* **1994**, *33*, 9–14. [CrossRef]

45. Colombo, M.G.; Gudel, H.U. Synthesis and high-resolution optical spectroscopy of bis[2-(2-thienyl)pyridinato-C3,N′](2,2′-bipyridine)iridium(III). *Inorg. Chem.* **1993**, *32*, 3081–3087. [CrossRef]

46. Ichimura, K.; Kobayashi, T.; King, K.A.; Watts, R.J. Excited-state absorption spectroscopy of ortho-metalated iridium(III) complexes. *J. Phys. Chem.* **1987**, *91*, 6104–6106. [CrossRef]

47. King, K.A.; Spellane, P.J.; Watts, R.J. Excited-state properties of a triply ortho-metalated iridium(III) complex. *J. Am. Chem. Soc.* **1985**, *107*, 1431–1432. [CrossRef]

48. Balton, C.B.; Murtaza, Z.; Shaver, R.J.; Rillema, D.P. Excited-state properties of platinum(II) complexes containing biphenyl as a ligand: Complexes of the type [(bph)PtL2], where L = monodentate or saturated bidentate ligands. *Inorg. Chem.* **1992**, *31*, 3230–3235.

49. Wong, W.Y.; Zhou, G.J.; Yu, X.M.; Kwok, H.S.; Tang, B.Z. Amorphous diphenylaminofluorene-functionalized iridium complexes for high-efficiency electrophosphorescent light-emitting diodes. *Adv. Funct. Mater.* **2006**, *16*, 838–846. [CrossRef]

50. Lakowicz, J.R. *Principles of Fluorescence Spectroscopy*, 3rd ed.; Springer: Berlin, Germany, 2006; 954p, ISBN 978-0-387-31278-1.

51. Eisinger, J. A variable temperature, UV luminescence spectrograph for small samples. *Photochem. Photobiol.* **1969**, *94*, 15–21.

52. Kasha, M. Paths of molecular excitation. *Radiat. Res.* **1960**, *2*, 243–275. [CrossRef] [PubMed]

53. Ge, G.; Zhang, G.; Guo, H.; Chuai, Y.; Zou, D. Yellow organic light-emitting diodes based on phosphorescent iridium(III) pyrazine complexes: Fine tuning of emission. *Inorg. Chim. Acta* **2009**, *362*, 2231–2236. [CrossRef]

54. Dragonetti, C.; Falciola, L.; Mussini, P.; Righetto, S.; Roberto, D.; Ugo, R.; Valore, A.; Angelis, D.F.; Fantacci, S.; Sgamellotti, A.; et al. The role of substituents on functionalized 1,10-phenanthroline in controlling the emission properties of cationic iridium(III) complexes of interest for electroluminescent devices. *Inorg. Chem.* **2007**, *46*, 8533–8547. [CrossRef] [PubMed]

55. De Angelis, F.; Fantacci, S.; Evans, N.; Klein, C.; Zakeeruddin, S.M.; Moser, J.E.; Kalyanasundaram, K.; Bolink, H.J.; Gratzel, M.; Nazeeruddin, M.K. Controlling phosphorescence color and quantum yields in cationic iridium complexes: A combined experimental and theoretical study. *Inorg. Chem.* **2007**, *46*, 5989–6001. [CrossRef] [PubMed]

56. Hasan, K.; Pal, A.K.; Auvray, T.; Zysman-Colman, E.; Hanan, G.S. Blue-green emissive cationic iridium(III) complexes using partially saturated strongly-donating guanidyl-pyridine/-pyrazine ancillary ligands. *Chem. Commun.* **2015**, *51*, 14060–14063. [CrossRef] [PubMed]

57. Gonzalez, I.; Dreyse, P.; Cortes-Arriagada, D.; Sundararajan, M.; Morgado, C.; Brito, I.; Roldan-Carmona, C.; Bolink, H.J.; Loeb, B. A comparative study of Ir(III) complexes with pyrazino[2,3-*f*][1,10]phenanthroline and pyrazino[2,3-*f*][4,7]phenanthroline ligands in light-emitting electrochemical cells (LECs). *Dalton Trans.* **2015**, *44*, 14771–14781. [CrossRef] [PubMed]

58. He, L.; Qiao, J.; Duan, I.; Dong, G.; Zhang, D.; Wang, L.; Qiu, Y. Toward highly efficient solid-state white light-emitting electrochemical cells: Blue-green to red emitting cationic iridium complexes with imidazole-type ancillary ligands. *Adv. Funct. Mater.* **2009**, *19*, 2950–2960. [CrossRef]

59. Sunahara, H.; Urano, Y.; Kijima, H.; Nagano, T. Design and synthesis of a library of BODIPY-based environmental polarity sensors utilizing photoinduced electron-transfer-controlled fluorescence ON/OFF switching. *J. Am. Chem. Soc.* **2007**, *129*, 5597–5604. [CrossRef] [PubMed]

60. Tomasi, J.; Persico, M. Molecular interactions in solution: An overview of methods based on continuous distributions of the solvent. *Chem. Rev.* **1994**, *94*, 2027–2094. [CrossRef]

61. Simkin, B.Y.; Sheikhet, I. *Quantum Chemical and Statistical Theory of Solutions—A Computational Approach*; Ellis Horwood: London, UK, 1995.

62. Frisch, M.J.E.A.; Trucks, G.W.; Schlegel, H.B.; Scuseria, G.E.; Robb, M.A.; Cheeseman, J.R.; Scalmani, G.; Barone, V.; Mennucci, B.; Petersson, G.A.; et al. *Gaussian 09, Revision D. 01*, Gaussian, Inc.: Wallingford, CT, USA, 2009.

63. Dooley, R.; Milfeld, K.; Guiang, C.; Pamidighantam, S.; Allen, G. From proposal to production: Lessons learned developing the computational chemistry grid cyberinfrastructure. *J. Grid Comput.* **2006**, *4*, 195–208. [CrossRef]

64. Milfeld, K.; Guiang, C.; Pamidighantam, S.; Giuliani, J. Cluster computing through an application-oriented computational chemistry grid. In Proceedings of the 2005 Linux Clusters: The HPC Revolution, NCSA University of Illinois, CHPC University of New Mexico and IBM, Chapel Hill, NC, USA, 25–28 April 2005.

65. Dooley, R.; Allen, G.; Pamidighantam, S. Computational chemistry grid: Production cyberinfrastructure for computational chemistry. In Proceedings of the 13th Annual Mardi Gras Conference, CCT, Louisiana State University, Baton Rouge, LA, USA, 3–5 February 2005; p. 83.